J. Fluid Mech. (1990), *vol.* 215, *pp.* 101–124
Printed in Great Britain

A visual study of the coherent structure of the turbulent boundary layer in flow with adverse pressure gradient

By QI XIANG LIAN

Institute of Fluid Mechanics, Beijing Institute of Aeronautics and Astronautics, Beijing 100083, China

(Received 24 April 1989 and in revised form 20 October 1989)

Experimental investigations were carried out on the coherent structures of turbulent boundary layers in flow with adverse pressure gradient and, in the vicinity of separation, extensive visual observations using hydrogen bubble technique have been performed. In a flow with adverse pressure gradient the size of the structures are larger, therefore more details were observed. By a suitable manipulation of the generation of hydrogen bubble time-lines some new results were obtained in observing plan views near the wall. (1) The long streaks downstream along the interface regions between low-speed and high-speed streaks are continually stretching and their velocity may be greater than that of high-speed streaks, and the hydrogen bubbles in the long streaks generally have a longer life. (2) The x, y-vortices (streamwise) were also observed along the interface regions between high-speed and low-speed streaks. (3) The z-vortices (transverse) were observed at the front of the high-speed regions.

1. Introduction

Since the discovery of low-speed streaks and bursting phenomenon in the near-wall region of turbulent boundary layers in the 1960s by Kline *et al.* (1967), many papers have been contributed to the investigations on coherent structures in turbulent boundary layers, as reviewed by Cantwell (1981) and Hussain (1983). Yet a consensus on the explanations or the detailed descriptions of the structures is still lacking (for example, see Kline & Falco 1980; Kim 1983). In the plan views observed using the hydrogen bubble technique in the wall region of turbulent boundary layers, there are many long streamwise streaks observable far downstream of bubble wire, as seen by various researchers (Kline *et al.* 1967; Nakagawa & Nezu 1981; Smith & Metzler 1983; Lian 1983; Johanson & Smith 1986). It seems this is a universal characteristic of the structure in the wall region. Yet the long streaks are rarely investigated: why they are so long, and how they are generated? As pointed out by Falco (Kline & Falco 1980) no answer is known. Usually the long streaks were regarded as a part of the low-speed streak, for example they were used for counting the spanwise spacing of low-speed streaks. The author noted that the low-speed streaks are much wider in flows with adverse pressure gradient than those with zero pressure gradient (Lian 1983). Therefore it is easier, in an adverse pressure gradient, to distinguish the flow inside a low-speed streak, and the flow at its interface with a high-speed streak. Inside either the low-speed or high-speed streaks, the flows are generally relatively uniform, chaotic flows appear usually only along the interface

or border regions. Thus further study of the interface region is needed. A better understanding of the structures of turbulent flow in the wall regions also is important for practical purposes. Considerable advancement in drag reduction investigations based on the understanding of coherent structures has been obtained in recent years (see Bushnell 1983; Guezennec & Nagib 1985; Blackwelder & Chang 1986). In the present investigation more attention is paid to the long streaks and x, y-vortices (streamwise) along the interface regions between streaks. By a simple manipulation of the duration of the generation of hydrogen bubbles, some important features of the long streaks and x, y-vortices (streamwise) have been revealed.

2. Experimental facilities and experimental procedures

The experiment was performed in a recirculating water channel. Water is pumped to a large settling tank with a thick porous sheet and three screens. There is a contraction cone connected to the test section. The test section is 6.8 m long, 0.4 m wide and 0.4 m deep, made of Plexiglas to facilitate visualization. A Plexiglas flat plate with a length of 6 m and a width of 0.4 m was set along one sidewall of the test section; its boundary layer was tripped at the leading edge. Observations were made at stations about 5 m from the leading edge. For the experiments on flows with adverse pressure gradient, a curved wall was set up along the other sidewall, opposite to this flat plate. A two-dimensional passage was formed between them. The shape of the divergent part of this passage is shown in figure 1. The entrance is located 5 m from the leading edge of the flat plate. The distribution of the divergence angle is designed according to the idea of Stratford (1959), such that it is largest at the beginning of the diffuser where the boundary layer is thinnest, and it decreases along the stream as the thickness of the boundary layer increases. Thus the flow may be maintained in the vicinity of separation. Small regions of reverse flow in the wall region may be observed frequently, yet full separation was avoided throughout the entire divergent passage. The free-stream velocity U and the Reynolds number based on the momentum thickness of the boundary layer along the divergent passage are shown in figure 1.

Observations were made along the middle of the flat plate at various x-stations ($x = 0$ at the diffuser entrance). Visual studies using the hydrogen bubble technique were performed. The platinum wire used for generating hydrogen bubbles is 0.025 mm in diameter; it is connected to the cathode of a pulsating current with adjustable frequency and adjustable voltage. The frequency preferred in the present experiment is around 8 to 14 Hz. The arrangement of the platinum wire and the illuminating light is shown in figure 2. The plan view of the structure is shown by the hydrogen bubbles generated from a transverse platinum wire normal to the free stream and parallel to wall. These arrangements are similar to those used by Kline *et al.* (1967).

3. Experimental results and discussion

3.1. *The time-mean velocity profiles*

Time-mean velocity profiles of the boundary layer were measured by a laser anemometer (DISA 55-X) at various x-stations along the flat plate in the divergent passage. The results are shown in figure 3. In the region from $x = 100$ mm to 500 mm there is an obvious inflection point in the velocity profile. The shape parameter H ($H = \delta^*/\theta$) is 2.1 at $x = 200$ mm, and 2.3 at $x = 300$ mm. These H-values are a little

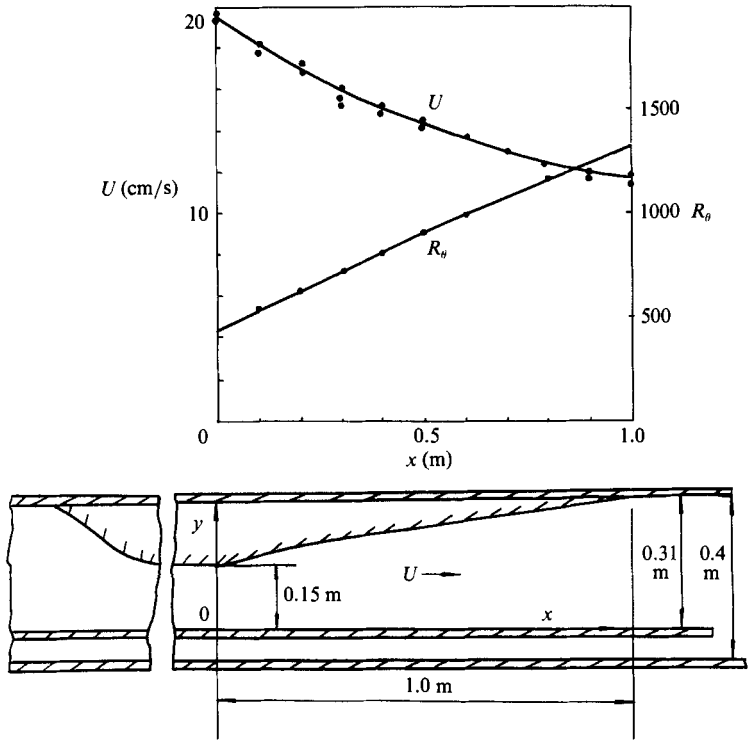

FIGURE 1. Sketch of the divergent passage and the flow parameters. U is the free-stream velocity, $R_\theta = U\theta/\nu$ is the Reynolds number based on the momentum thickness of the boundary layer.

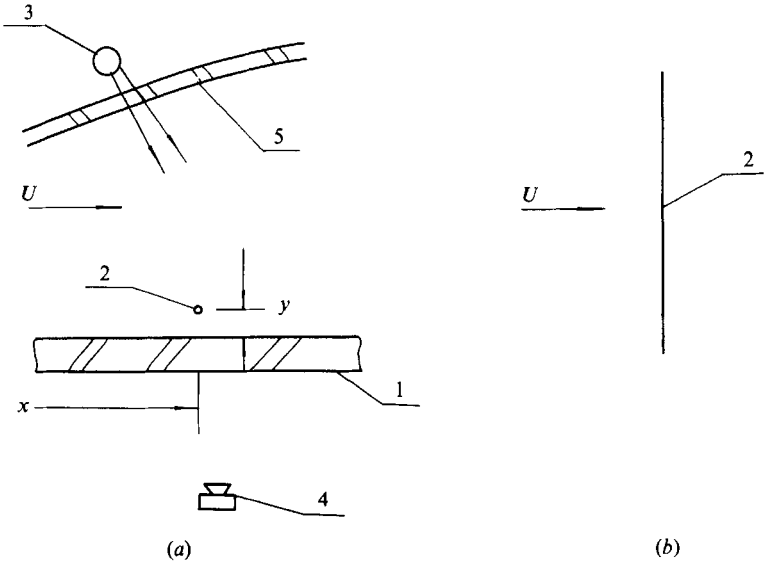

FIGURE 2. Arrangement of the transverse platinum wire for visualizing plan views. (*a*) Top view: (1) the flat plate, (2) platinum wire, (3) illuminating light, (4) camera, (5) curved wall. (*b*) The side view.

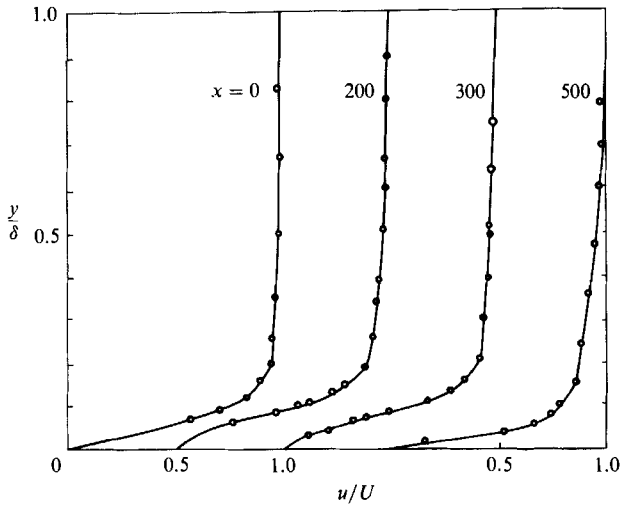

FIGURE 3. The time-mean velocity profiles of the boundary layer along the flat plate in the divergent passage (Lian 1985).

smaller than those for the separation criterion of Sandborn & Kline (1961). There are only small reverse-flow regions observed intermittently in this region on the hydrogen bubble visualized flow pictures. Thus the flow is characteristic of the incipient stage of separation in the turbulent boundary layer. In the present paper the experimental results discussed are primarily in the region from $x = 100$ mm to 500 mm, where the boundary layer is in incipient separation. Simpson, Strikland & Barr (1977), and Simpson, Chew & Shivaprasad (1981) performed experiments on a turbulent boundary layer in the vicinity of separation in a wind tunnel diffuser; however, the downstream part of the flow was fully separated, and the shape parameter H reached 4.6. Therefore Simpson *et al.*'s flow is somewhat different from that of the present experiment. Nevertheless, some features may be similar, for example the bursting period in both experiments becomes longer (Simpson *et al.* 1977; Lian 1985).

3.2. *Plan view*

As pointed out by Kline & Falco (1980) and many other authors the low-speed streaks, high-speed streaks and long streaks on the plan views in the wall region are universal features of coherent structures for known examples of turbulent boundary layers. In the flow with zero pressure gradient the low-speed streaks appear as narrow streaks while the high-speed streaks are much wider, as shown by Kline *et al.* (1967) and Smith & Metzler (1983). In the flow with adverse pressure gradient, especially in incipient separation, the low-speed streaks become much wider; their width may be comparable with that of the high-speed streaks (Lian 1983). Therefore it is possible to observe some features inside the low-speed streaks. As shown by Lian (1983), the flow inside a low-speed streak, similar to the flow inside a high-speed streak, is relatively uniform and quiet. Chaotic flow occurred mainly along the interface between a low-speed and high-speed streak; a typical example is shown in figure 4. Therefore, the interface regions may play an important role in producing turbulence. In the present investigation attention is directed towards the observation of the long streaks and vortices in the interface regions.

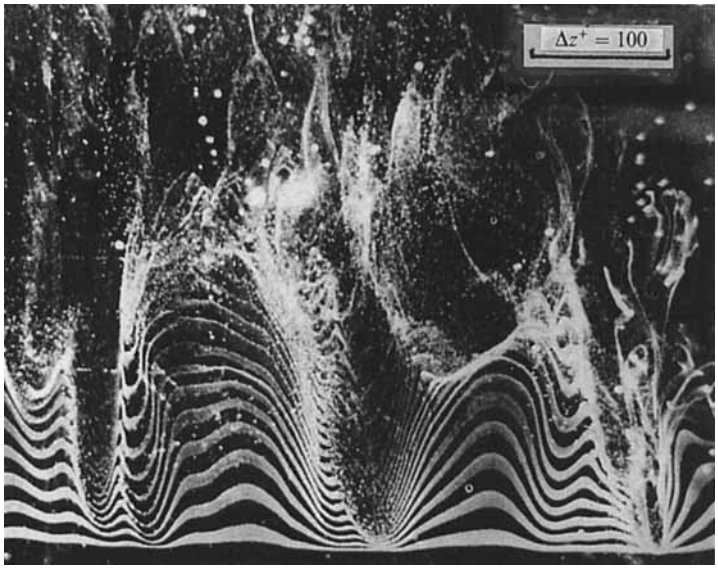

FIGURE 4. A typical plan view of the turbulent boundary layer at $x = 200$ mm and $y^+ = 12$, showing that the low-speed streaks are relatively wide.

3.3. *Long streaks*

A remarkable feature common to all near-wall plan views of various turbulent boundary layers recorded is the very long streaks formed by hydrogen bubbles; they are visible very far downstream, and the hydrogen bubbles in these long-streaks exist a long time after all hydrogen bubbles in the high-speed and low-speed streaks have vanished. Why are there always these long streaks? Why do they remain visible so far downstream? Why do the hydrogen bubbles in them exist so long? These questions are interesting but not explained yet. Efforts were made in this experiment to clarify these questions, and two new simple methods were used.

Method (A) Cut off the electric current, wait for a while until nearly all hydrogen bubbles disappear in the plan view, then turn on both the electric current and the motion picture camera simultaneously. At the beginning, the hydrogen bubble time-lines are nearly parallel to the platinum wire, and are almost straight lines. A few frames later, low-speed streaks and high-speed streaks begin to appear on the motion picture film, and almost at the same time narrow streaks begin to protrude downstream from some of the interface regions between high- and low-speed streaks as shown in figure 5. Since there are no hydrogen bubbles downstream of the leading marks, it is easy to see where the flow speed is higher. The narrow streaks just mentioned obviously have greater velocity than their neighbouring high-speed streaks, as the high-speed streaks lag behind them. These narrow streaks afterwards grow quite long. In the photographs visualized by usual method, it is difficult to distinguish whether the long streaks or the high-speed streaks have higher velocity, because the hydrogen bubble time-lines are mixed together along the long streaks as shown in figure 4. The photographs taken by Kline *et al.* (1967), Nakagawa & Nezu (1981), Smith & Metzler (1983) and Lian (1983) show the same feature. Since there is no suitable mark on a long streak for comparing its speed with high-speed streak, it is difficult to observe the protrusion of the markers from the interface region and the formation process of the long streaks in all these experiments.

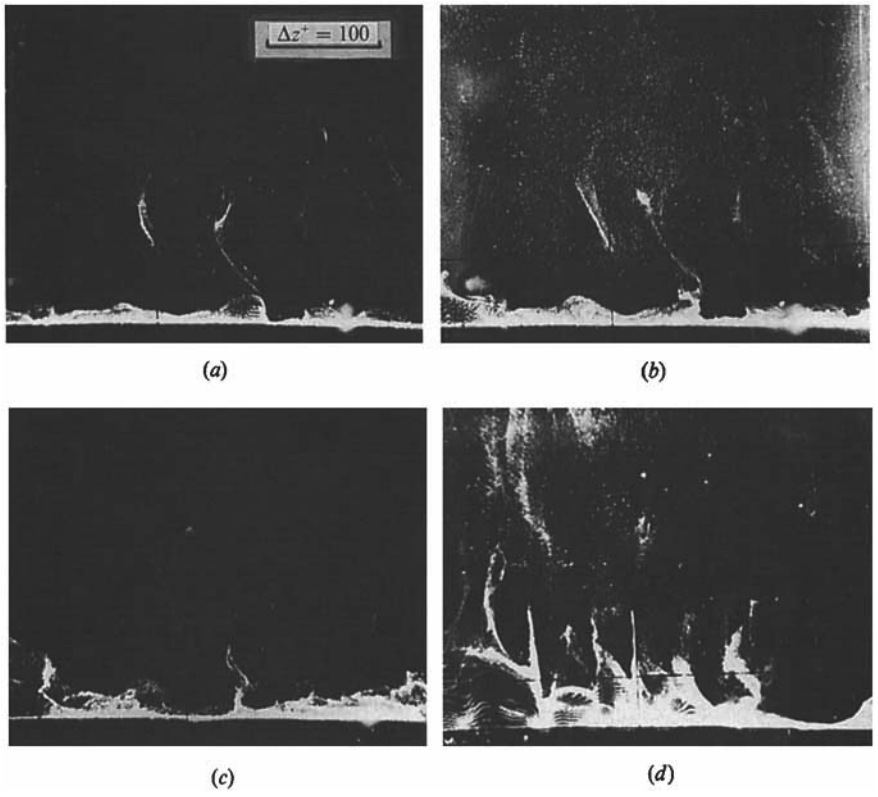

FIGURE 5. Photographs show the generating process of long streaks: (*a*) $x = 500$ mm, $y^+ = 2.5$, $t = 0$; (*b*) $x = 500$ mm, $y^+ = 2.5$, $t = 0.5$ s; (*c*) $x = 500$ mm, $y^+ = 2.5$, $t = 1.25$ s; (*d*) $x = 300$ mm, $y^+ = 2$, $t = 3.5$ s.

Method (B). Cut off the electric current for a while, until all high-speed and low-speed streaks vanish on the visualized picture, then turn on the electric current. After a small time interval, when several hydrogen bubble time-lines have been released, cut off the electric current again. By this method it is easy to observe the stretching of the interface regions, and the formation and stretching of the long streaks. In figure 6(*a*), $t = 0$, there is a very dense white line near the platinum wire. It is several hydrogen bubble time-lines just released; they are so close to each other that they look like a single wide white line. The platinum wire is located at $x = 100$ mm and $y^+ = 2.5$. Far downstream there are some dilute white long streaks which are the remnants of the previously visualized long streaks. In figure 6(*b*), $t = 0.5$ s, some high-speed and low-speed streaks begin to appear; they have developed from the wide white line mentioned above. In figure 6(*c*), $t = 1$ s, and figure 6(*d*), $t = 1.5$ s, long streaks begin to form and protrude downstream along the interface between high- and low-speed streaks. The hydrogen bubble time-lines in the high-speed streaks gradually become dilute. In figure 6(*e*), $t = 2.125$ s, many interfaces have long streaks. They are only at the initial stage, and are not very long, but they are stretching; their downstream parts are almost parallel to the free stream. Figures 7(*a*) to 7(*c*) were visualized by the same method; they were taken at $t = 2.25$ s, 2.75 s and 3.1875 s respectively. The platinum wire is at $x = 100$ mm and $y^+ = 5$. A similar flow pattern is shown in the photographs. The elongated long streaks along the interface regions appear still dense white, while most of the high-speed streaks and

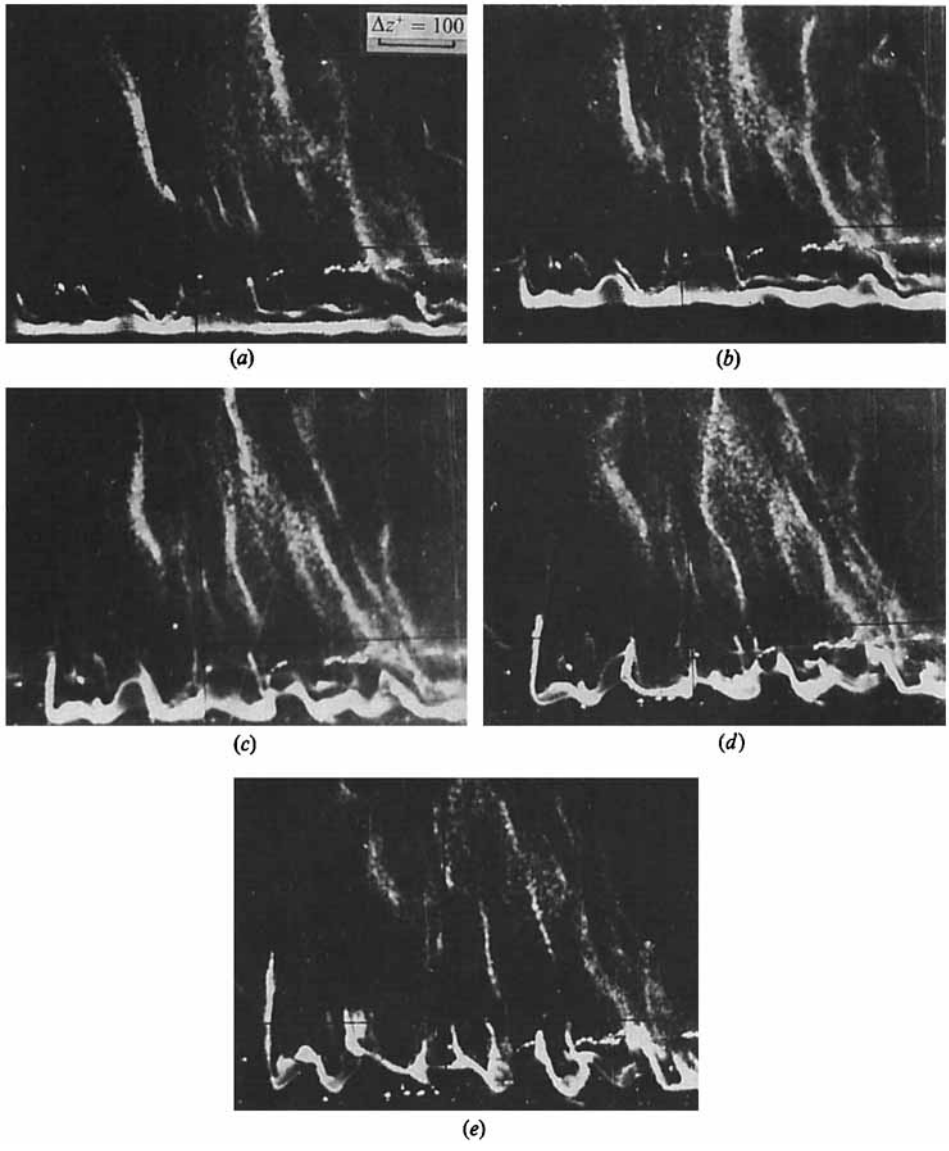

FIGURE 6. Photographs show the generation and stretching of the long streaks, $x = 100$ mm, $y^+ = 2.5$: (*a*) $t = 0$, (*b*) 0.5 s, (*c*) 1.0 s, (*d*) 1.5 s, (*e*) 2.125 s.

some low-speed streaks appear dilute white. In figure 8 the photographs were taken at $x = 500$ mm and $y^+ = 10$. Since y^+ is larger, the hydrogen bubble time-lines have greater spacing, and the high- and low-speed streaks are visualized clearly. In figure 8(*b*) the l shows a low-speed streak which is very near to separation so that all hydrogen bubbles are closed together and look like a single line. The local velocity must be nearly zero. In figure 8(*b*), $t = 0.688$ s and figure 8(*c*), $t = 0.875$ s, a pair of x-vortices is rolling up along the interface regions, marked v. In figure 8(*d*), $t = 1.063$ s, these x-vortices become very distinct, the winding and overlapping of the hydrogen bubble time-lines along streamwise direction is clearly visible. In figures 8(*e*) and 8(*f*), $t = 1.625$ s and 2.125 s respectively almost all the hydrogen bubble lines in the high- and low-speed streaks have vanished; however, vortices remain

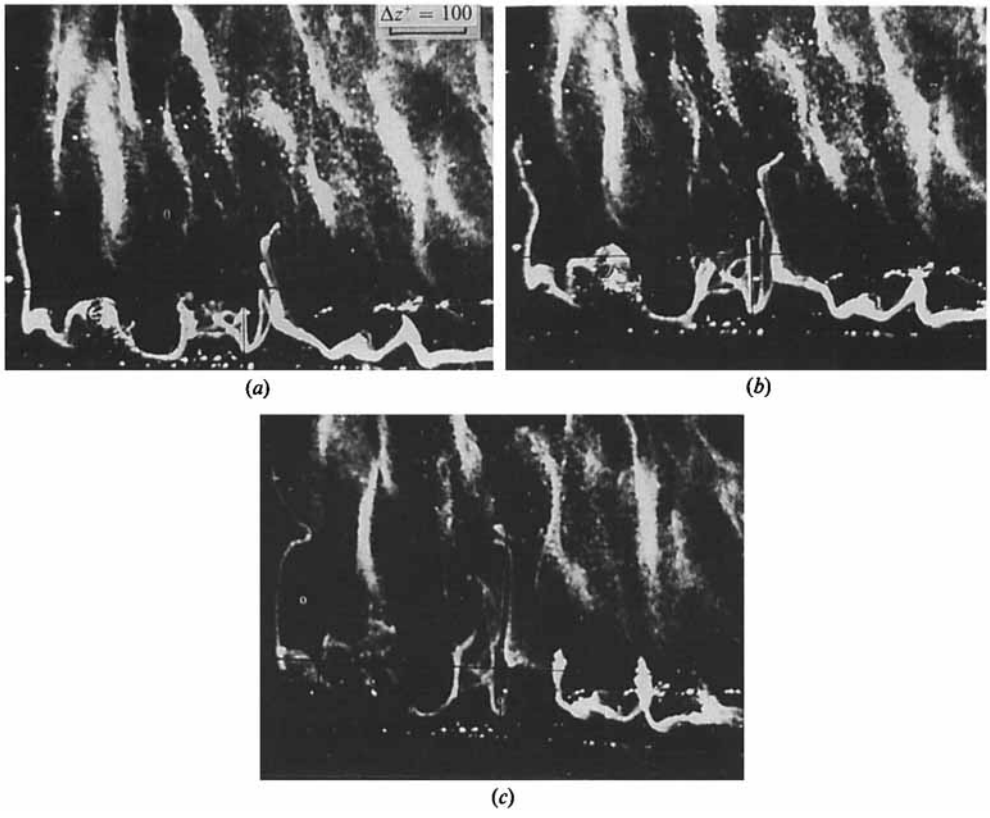

FIGURE 7. Photographs show the generation and stretching of the long streaks, $x = 100$ mm, $y^+ = 5$: (*a*) $t = 2.25$ s, (*b*) 2.75 s, (*c*) 3.1875 s.

dense white on the photograph. There is remarkable stretching of the length of the x-vortex just mentioned between figures 8(*b*) and 8(*f*). At the same time, the streamwise length of the high- and low-speed streaks in these figures remains almost unchanged. The variation of the length of the x-vortex (streamwise) marked v was measured from motion picture films; the result is plotted in figure 9. The streamwise length of a nearby high-speed streak, marked h in figure 8, was also measured and is also shown in figure 9.

The spanwise spacing values of the long streaks and low-speed streaks were measured from the motion picture films using visual identification. The identification of the long streaks was generally straightforward. Using method A or B, more than 2 to 3 s after the turning off the electric current, there are many streaks with concentrated hydrogen bubbles protruding in the downstream direction along the interface regions between the high-speed and low-speed streaks. These protruding streaks were used for counting the spacing of long streaks. Those streaks which did not satisfy the criterion $(x_f - x_h)/x_h \geqslant 0.2$ were neglected, where x_f is the distance of the fore end of the protruding streaks to the platinum wire, and x_h is the distance of the leading hydrogen bubble time-line of the neighbouring high-speed streak to the platinum wire. Generally very few streaks were neglected. Another method was used for counting the spacing of the long streaks; using the above method B, about 10 s after turning off the electric current, mainly the long streaks remain in the plan view. This is shown typically in the downstream region in figure 7. A bubble line inclined

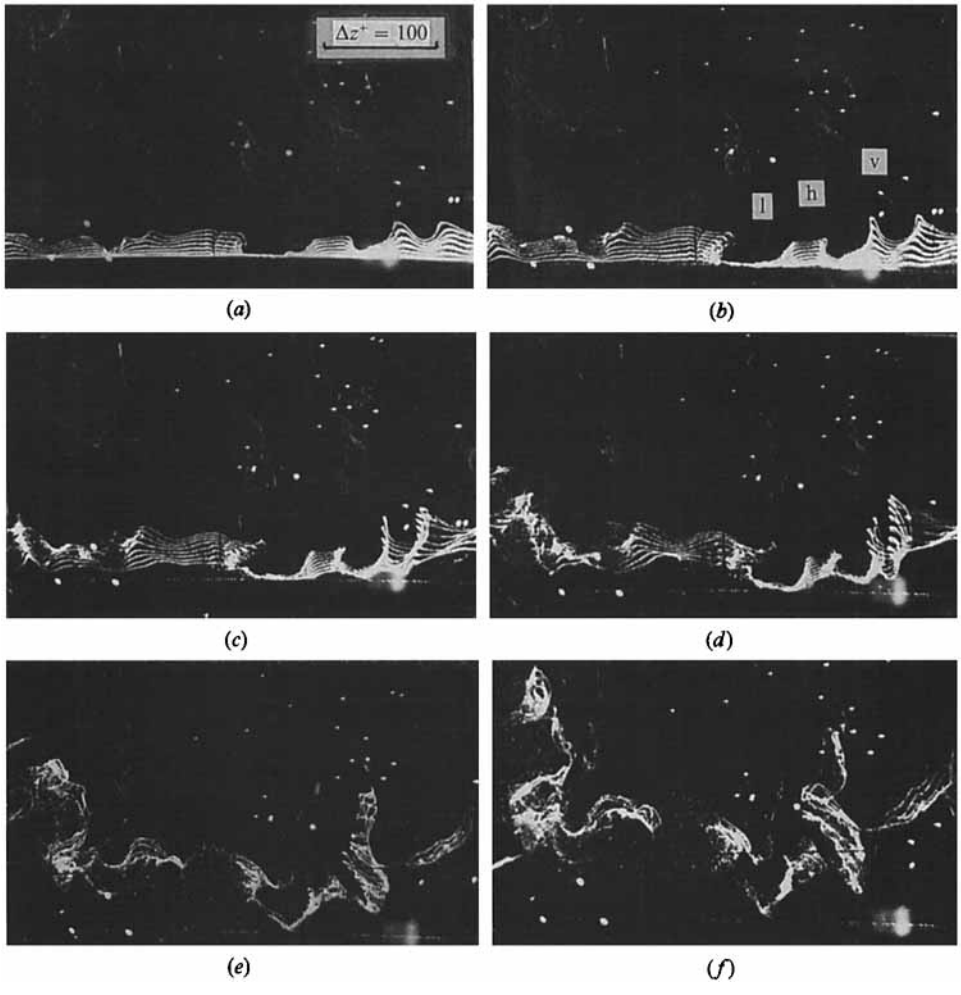

FIGURE 8. Photographs show the stretching of two x-vortices along the interface region between a high-speed and low-speed streak, $x = 500$ mm, $y^+ = 10$: (*a*) $t = 0.25$ s, (*b*) 0.688 s, (*c*) 0.875 s, (*d*) 1.063 s, (*e*) 1.625 s, (*f*) 2.125 s.

less than 30° to the x-axis is defined as a streamwise bubble line, and a streamwise bubble line longer than 100 wall units is defined as a long streak. No long streak of incline greater than 45° was observed in the experiment, and an inclination greater than 30° was rare. Sometimes a part of the long streak might be inclined greater than 30°, but this part was generally far shorter than the total length of the long streak. In measuring the spacing of the long streaks, only the main segment of the long streak whose inclination was less than 30° was considered. The spanwise spacing value between two long streaks generally varies along the x-direction. At least five measurements distributed along the x-direction were made for each spacing between two long streaks. The results of these two methods are essentially the same. Low-speed streaks were also identified from plan views using method B. About two seconds after turning off the electric current, the rear-most hydrogen bubble time-line forms a wavy curve as shown typically in figures 6(*d*), 6(*e*), 7(*a*) and 7(*b*). There are many segments convex to the platinum wire in each rear hydrogen bubble time-line. Each convex segment corresponds to a local low-speed region. The minimum

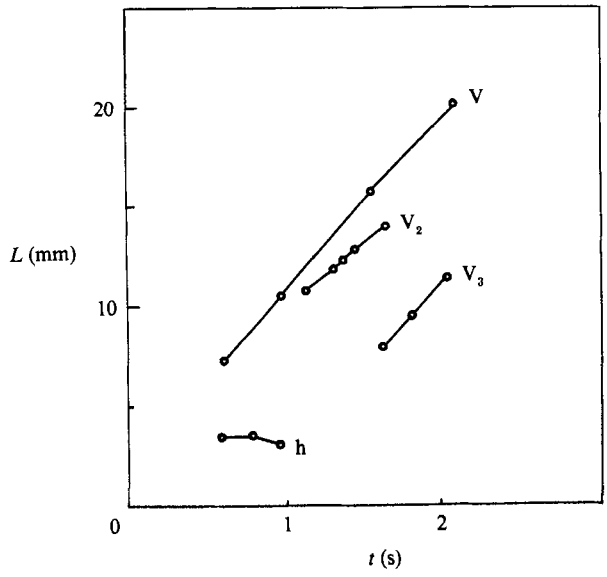

FIGURE 9. The stretching of a streamwise vortex (V) a high-speed streak (h in figure 8) and streamwise vortices (V_2 and V_3 in figure 13).

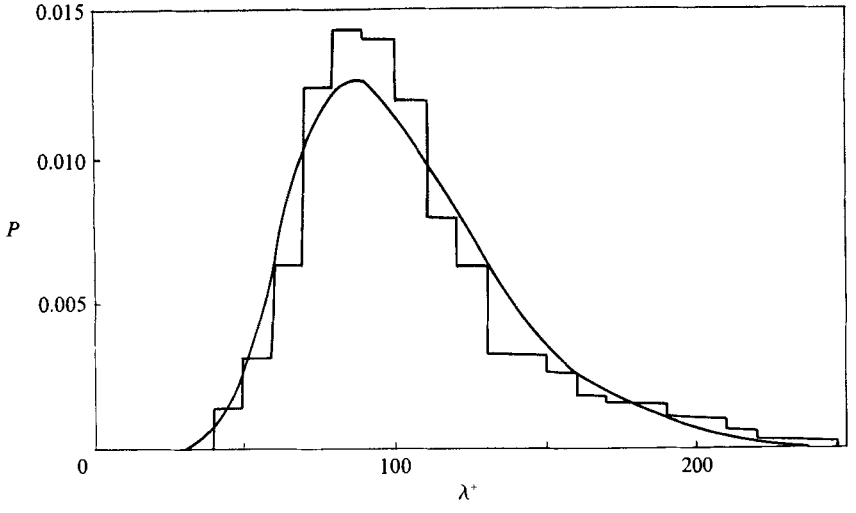

FIGURE 10. The histograms of the spanwise spacing of the long streaks in the plan views at $x = 100$ mm and $y^+ = 5$. $n = 412$, $\bar{\lambda}^+ = 104$, $\lambda_m^+ = 85$, $s = 0.35$.

points of such convex segments were taken for measuring spanwise spacing values of low-speed streaks. Generally there is no confusion in the identification of low-speed streaks by this method. In a few cases very narrow convex segments may appear in a wide high-speed streak, or concave segments in a low-speed region, thus the identification may be confused. Let u_n be the velocity inside this narrow region, and u be the velocity in the neighbouring streak. Then if $|u_n - u|/u \leqslant 0.3$, the narrow region is neglected for measuring the spacing of low-speed streaks. The distances of the rear hydrogen bubble time-lines to the platinum wire are proportional to the local flow velocity, so that they were used for measuring u_n and u. This criterion is the same as that used by Smith & Metzler (1983). The histograms of the spacing of the

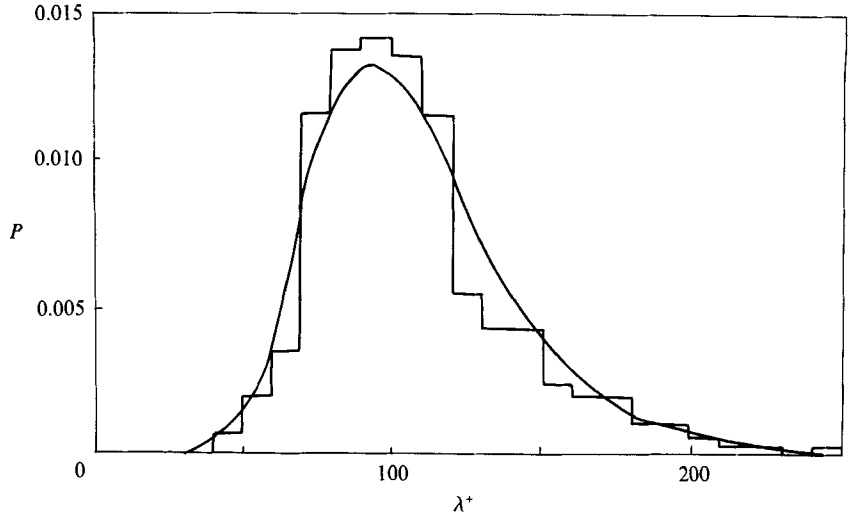

FIGURE 11. The histogram of the spanwise spacing of the low-speed streaks in the plan views at $x = 100$ mm and $y^+ = 5$. $n = 285$, $\bar{\lambda}^+ = 107$, $\lambda_m^+ = 95$, $s = 0.32$.

long streaks and low-speed streaks are shown in figures 10 and 11. They were obtained from the plan views visualized with the platinum wire located at $x = 100$ mm and $y^+ = 5$. The solid line in these figures is the lognormal probability density function $P(\lambda^+)$, defined in the following:

$$S = \left[\sum_{i=1}^{n} (\lambda_i^+ - \bar{\lambda}^+)^2/(n-1)\right]^{0.5}, \tag{1}$$

$$s = S/\bar{\lambda}^+, \tag{2}$$

$$A = \bar{\lambda}^+/(1+s^2)^{0.5}, \tag{3}$$

$$B = [\ln(1+s^2)]^{-0.5}, \tag{4}$$

$$P(\lambda^+) = B\exp[-\tfrac{1}{2}\{B\ln(\lambda^+/A)\}^2]/(2\pi)^{0.5}\lambda^+, \tag{5}$$

where λ^+ is the measured spacing value in wall units, and $\bar{\lambda}^+$ is the average value of λ^+, S is the standard deviation of the measurements, s is the coefficient of variation, and n is the number of samples. The histograms of the low-speed streaks and the long streaks are essentially similar. The average spacing of low-speed streaks is a little larger than that of the long streaks. Generally, a low-speed streak generates only one long streak at one of its interfaces with a high-speed streak. But sometimes two long streaks were generated, as shown in figure 6(*e*). Also some poorly developed low-speed streaks did not generate any long streaks but such poorly developed low-speed streaks were generally neglected in counting the spanwise spacing according to the above criterion. The coefficient of variations lies between 0.3 and 0.4; this is in agreement with the values measured by Smith & Metzler (1983) in the flow with zero pressure gradient.

The most probable value of the spacing λ_m^+ is the value where $P(\lambda^+)$ is maximum. This is obtained by solving the equation

$$\mathrm{d}P/\mathrm{d}\lambda^+ = 0.$$

The result is

$$\lambda_m^+ = \bar{\lambda}^+(1+s^2)^{-1.5}. \tag{6}$$

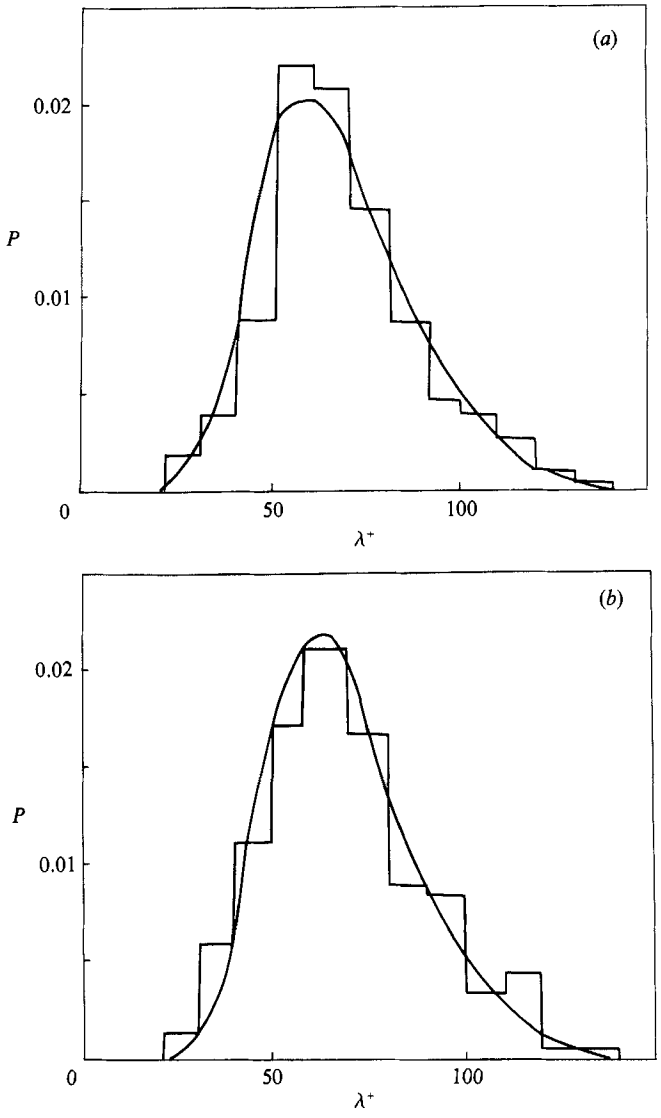

FIGURE 12. The histograms of the spanwise spacing of the long streaks and low-speed streaks in the plan views at $x = 300$ mm and $y^+ = 5$: (*a*) long streaks, $n = 406$, $\bar{\lambda}^+ = 68$, $\lambda_m^+ = 59$, $s = 0.32$; (*b*) low-speed streaks, $n = 351$, $\bar{\lambda}^+ = 69$, $\lambda_m^+ = 60$, $s = 0.31$.

From the data of figure 10, s = 0.352, $\bar{\lambda}^+ = 104$, thus $\lambda_m^+ = 87.2$, and the most probable value in the histogram is 85. From the data of figure 11, $s = 0.315$, $\bar{\lambda}^+ = 107$, $\lambda_m^+ = 92.9$, the most probable λ^+ is 95 in the histogram. The discrepancy is small, as the number of samples is limited. The histograms of the spacing of the long streaks and the low-speed streaks at $x = 300$ mm and $y^+ = 5$ are shown in figure 12; they are similar to figures 10 and 11. The variations in the spanwise spacing values (in absolute length) of long streaks and low-speed streaks along the streamwise direction are small from $x = 100$ mm to 500 mm. For $y^+ = 5$, at $x = 100$ mm the average spanwise spacing of long streaks is 20.6 mm, at $x = 300$ mm it is 21.9 mm, and at $x = 500$ mm it is 22.2 mm. The average spanwise spacing values of the low-speed streaks are 21.5 mm, 22.3 mm and 23 mm respectively. Owing to the streaky nature

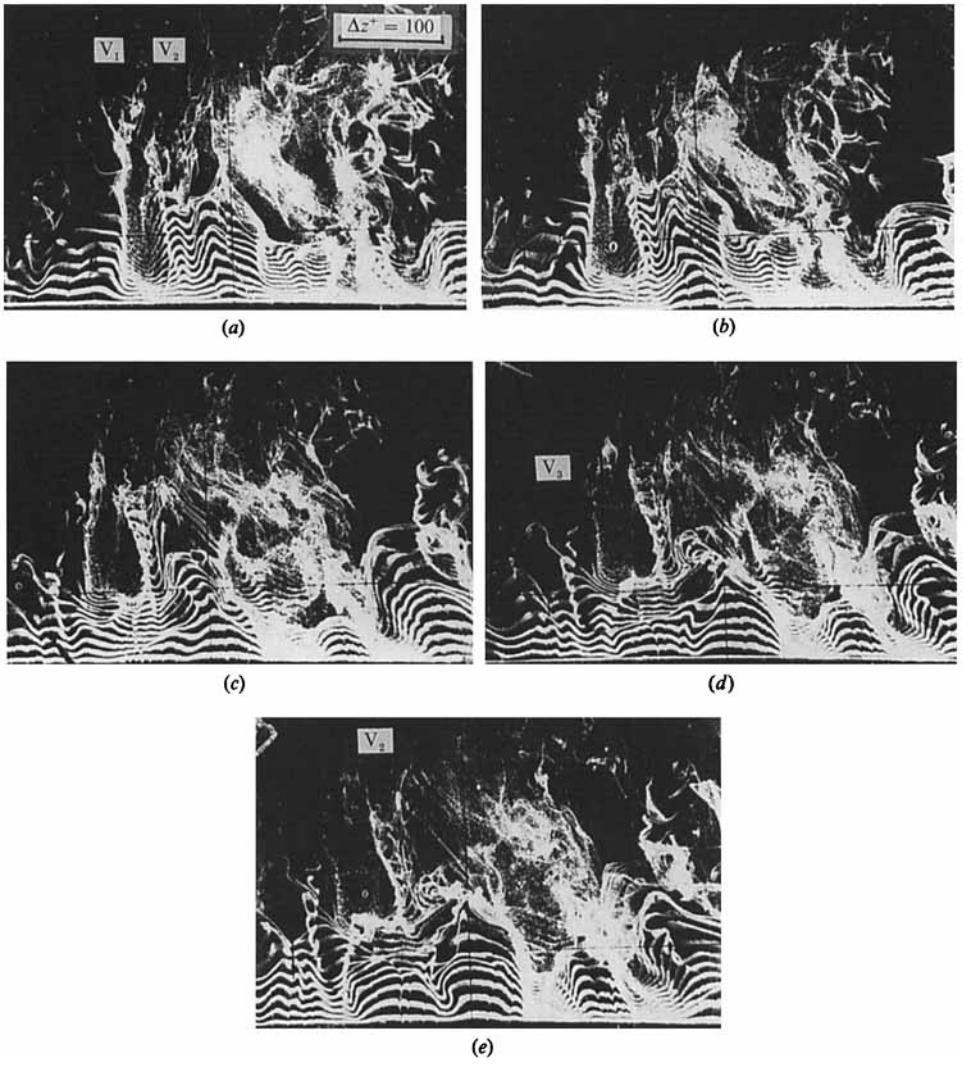

FIGURE 13. Photographs show stretching of streamwise vortices along the interface regions between high- and low-speed streaks at $x = 300$ mm and $y^+ = 11$: (*a*) $t = 0$, (*b*) 0.375 s, (*c*) = 0.75 s, (*d*) = 0.9375 s, (*e*) 1.3125 s.

of the structures in the wall region, the downstream spanwise spacing of the long streaks and low-speed streaks is influenced by the spacing of the upstream streaks, so that the variation of the spanwise spacing is small from $x = 100$ mm to 500 mm. As the wall stress is decreasing along the stream, the spacing of these streaks is decreased if expressed in wall units. The average spanwise spacing wall units at $x =$ 500 mm is 64.6 for long streaks, and 67 for the low-speed streaks.

3.4. *Streamwise vortex* (*x- or x, y-vortex*)

Streamwise vortices along interfaces between low-speed and high-speed streaks appear frequently in the wall-region plan views at $y^+ \sim 10$–20. The streamwise vortices are usually stretching. Sometimes a streamwise vortex forms a long streak downstream. An example is shown in the photographs in figure 13, taken at $x =$

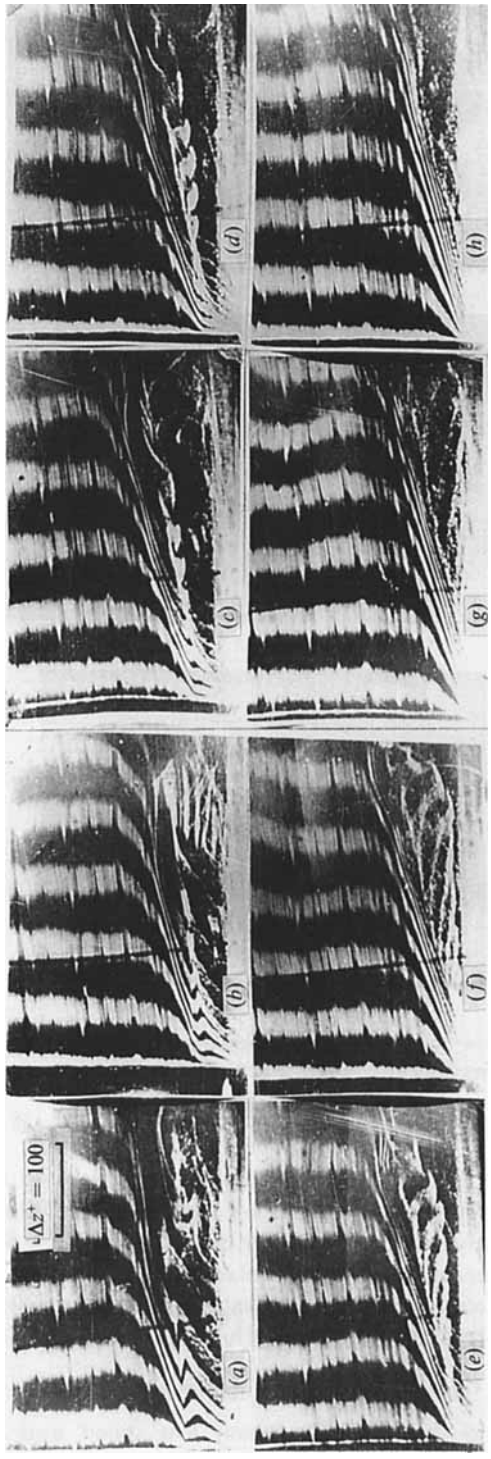

FIGURE 14. Photographs show side views of a large streamwise vortex, with the platinum wire located at $x = 200$ mm. The time interval between two photographs is 0.167 s (Lian 1985).

300 mm and $y^+ = 11$. In figure 13(*a*) the long streak marked V_1 is the remnant of a previous streamwise vortex, and an x-vortical shape marked V_2 is becoming visible. In figure 13(*b*), the bubbles at V_2 are still rolling up, showing a vortex. In figures 13(*c*) and 13(*d*), the vortical shape of the flow at V_2 becomes very evident; hydrogen bubble time-lines along this interface are winding around an almost straight and streamwise axis. The remnant of vortex V_1 becomes a long streak extending far downstream, and another streamwise vortex is becoming visible, marked V_3. In figure 13(*e*) the bubbles at V_3 are elongated and those at V_2 protrude far downstream; the bubbles at V_2 now appear as a long streak. The stretching of vortices V_2 and V_3 were also measured from motion picture films, and the lengths of the marker streaks are shown in figure 9.

Streamwise vortices can also be observed in the side views visualized by hydrogen bubble time-lines generated from a platinum wire normal to wall. Figure 14 shows side views of a large (x, y)-vortex with the platinum wire located at $x = 200$ mm. At the beginning, in the wall region and near to the platinum wire the spacing between the hydrogen bubble time-lines is very narrow; this implies that a low-speed streak is being made visible in the near-wall region. It seems that the hydrogen bubbles makes visible an interface. These hydrogen bubble time-lines rotate around a streamwise vortex along the interface and make it visible. In figures 14(*e*) and 14(*f*) the downstream segment of this vortex is lifted up and bent at about 45° to the wall and forms an (x, y)-vortex; this is a feature of a leg vortex element. From this picture one cannot tell if the leg element is isolated or is a portion of a larger vortical structure. In figure 14, two additional features are worth noting: (1) the vortex element is tilted with respect to the wall with the downstream end at higher y^+; (2) the apparent diameter marked by hydrogen bubbles increases downstream as y^+ increases along the vortex element. Feature (1) (tilting) is inherently masked in a plan view, and so plan views should therefore not be interpreted as showing accurate streamwise vortex orientation. Feature (2) (increase in diameter) is visible in some of the vortex elements shown in plan view (see figures 8 and 13), see also the discussion concerning figures 19, 20 and 21 below.

Figure 15 shows another example of a structure inclined in the (x, y)-direction, at about 45° to the wall. These photos were visualized by a laser light sheet in the (x, y)-plane, and the hydrogen bubbles were generated by a transverse platinum wire located at $x = 300$ mm and $y^+ = 8$. The arrangement is the same as for visualizing the usual plan views, only the illuminating light is a laser light sheet. The light sheet cuts the plan view in a narrow strip, and the camera shows a side view. In figure 15, the white dash segments are the hydrogen bubble time-lines cut by the light sheet. From the spacing of these dash segments, it can be deduced whether the local flow corresponds to a low-speed streak or a high-speed streak. In figure 15(*a*), the hydrogen bubble time-lines appear as the dash segments close to the wall. (At the bottom in these photographs there are also fainter dash segments, they are the images of the upper dash segments reflected by the test plate.) From the spacing of the dash segments the local velocity can be estimated. In figure 15(*a*) these segments appear like the cross-section of a high-speed streak. These photos again provide some evidence that in the low- and high-speed streaks the flow is smooth and quiescent, as the dash lines are smooth before they are lifted up. Figures 15(*b*) to 15(*d*) show the hydrogen-bubble-marked fluid lift-up from the wall region. Comparing figures 15(*a*) and 15b), one can see that the near-wall dash segments in figure 15(*a*) remain close to the wall, they do not lift up. The lifted fluid in figures 15(*b*) to 15(*d*) is coming from the neighbouring region outside the laser light sheet. It seems that there is an (x, y)-

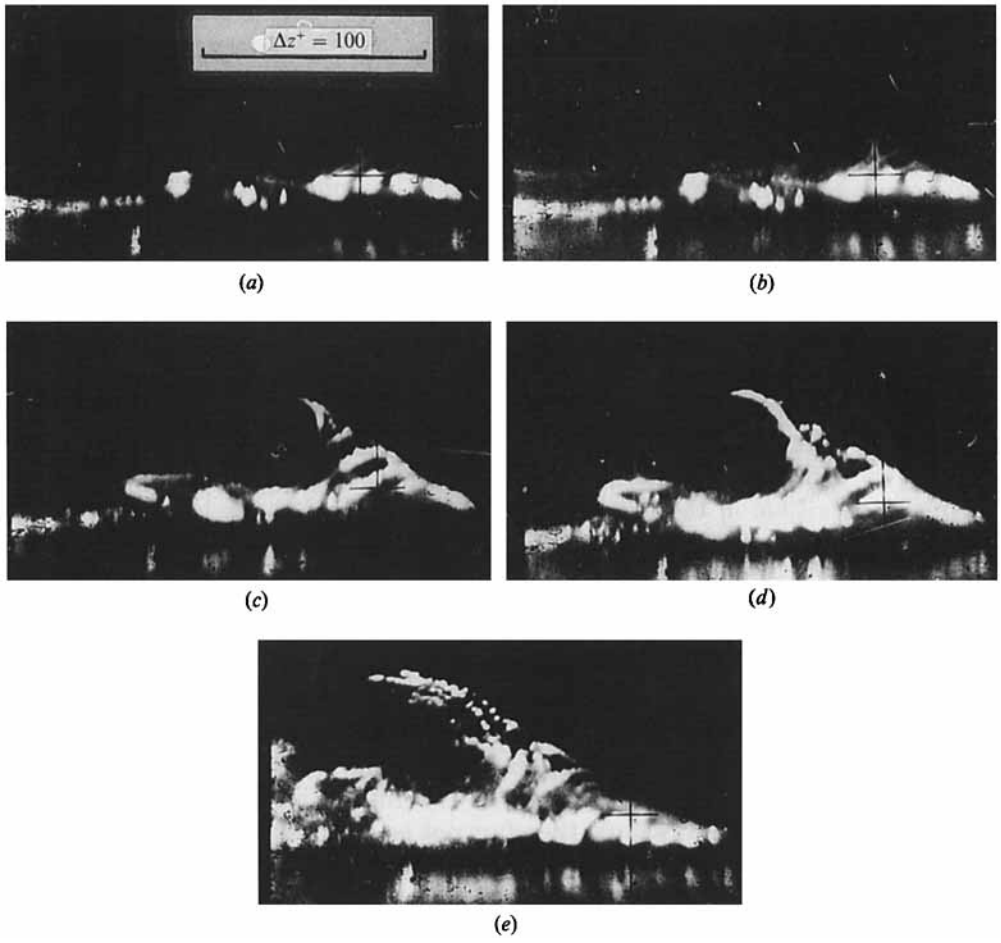

FIGURE 15. Photographs show side views visualized by a laser light sheet lying in the (x, y)-plane, and the hydrogen bubble lines are generated by a transverse platinum wire at $x = 300$, $y^+ = 8$. (*a*) $t = 0$, (*b*) 0.25 s, (*c*) 0.5 s, (*d*) 0.75 s, (*e*) 1.0 s.

vortex, and the lifted hydrogen-bubble-marked fluid appears as a vortex inclined at about 45° to the wall. The photos obtained by this technique show that most of the lifted up hydrogen-bubble-marked fluid structures are similar to figure 15. From motion picture films taken by this method, the periods of the lift-up of the hydrogen-bubble-marked fluid from the wall region may be counted, and the results are presented in figure 16. The average characteristic time of a cycle is 2.78 s.

3.5. *Transverse vortex* (*z-vortex*)

The transverse vortices can also be observed in plan views. They generally appear at the front of a high-speed region. The front of a high-speed region is wide in the z-direction and narrow in the x-direction. Downstream of it is a low-speed region, and upstream of it is a high-speed region. An example is shown in figure 17 (*a*) marked V, where there is a narrow region where the spanwise bubble lines are very close to each other; that is the front of a high-speed region. The bubble lines upstream of the front have higher velocity. The downstream bubble lines have lower velocity, and therefore are gradually overrun by the upstream bubble lines; this process is shown

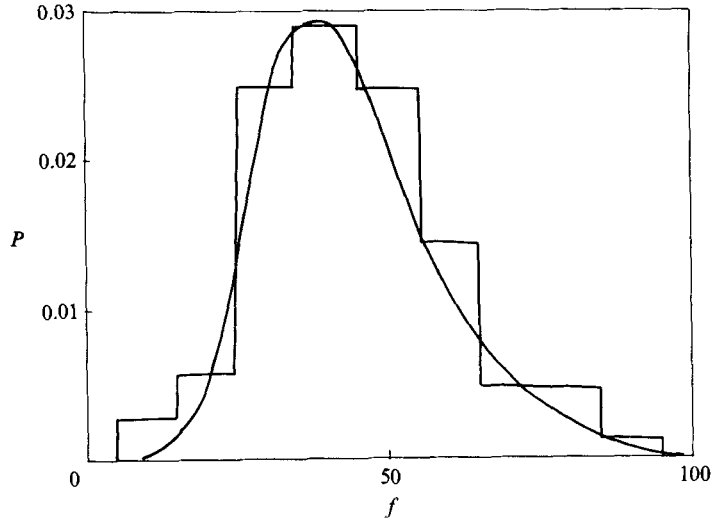

FIGURE 16. The histogram of the periods of the cyclical lift-up of the near-wall hydrogen bubble lines generated at $x = 300$ mm. Here, f is the number of frames of film between two lift-ups, $\bar{f} = 44.6$ frames; the average period $t = 2.78$ s, and $s = 0.345$, $n = 150$.

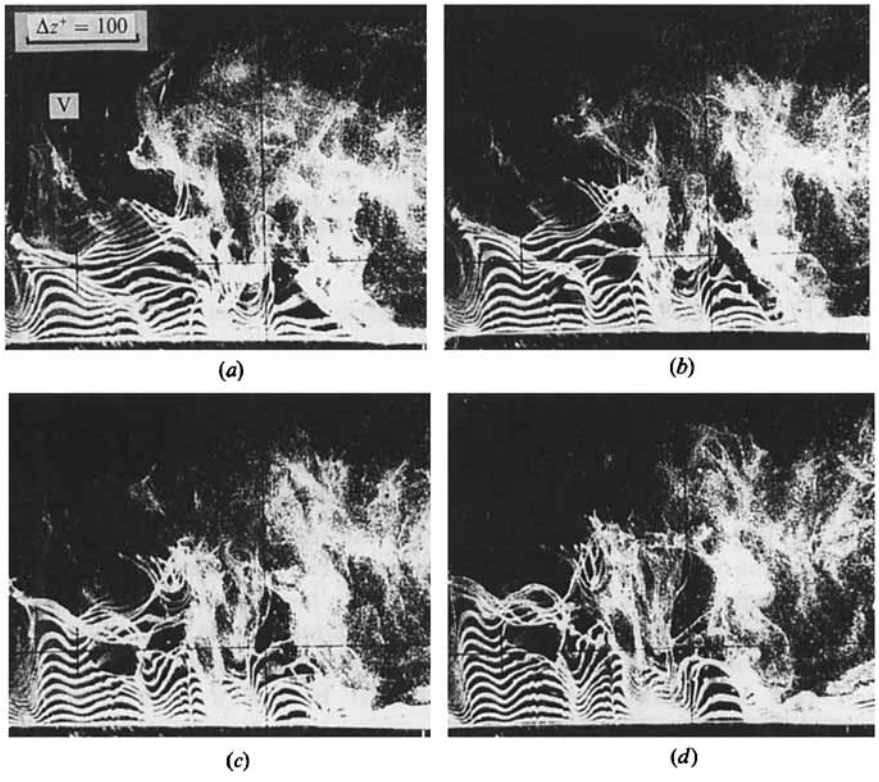

FIGURE 17. A z-vortex (transverse) visualized at the front of a high-speed region, marked V; $x = 300$ mm, $y^+ = 11$; (*a*) $t = 0$, (*b*) 0.1875 s, (*c*) 0.375 s, (*d*) 0.5625 s.

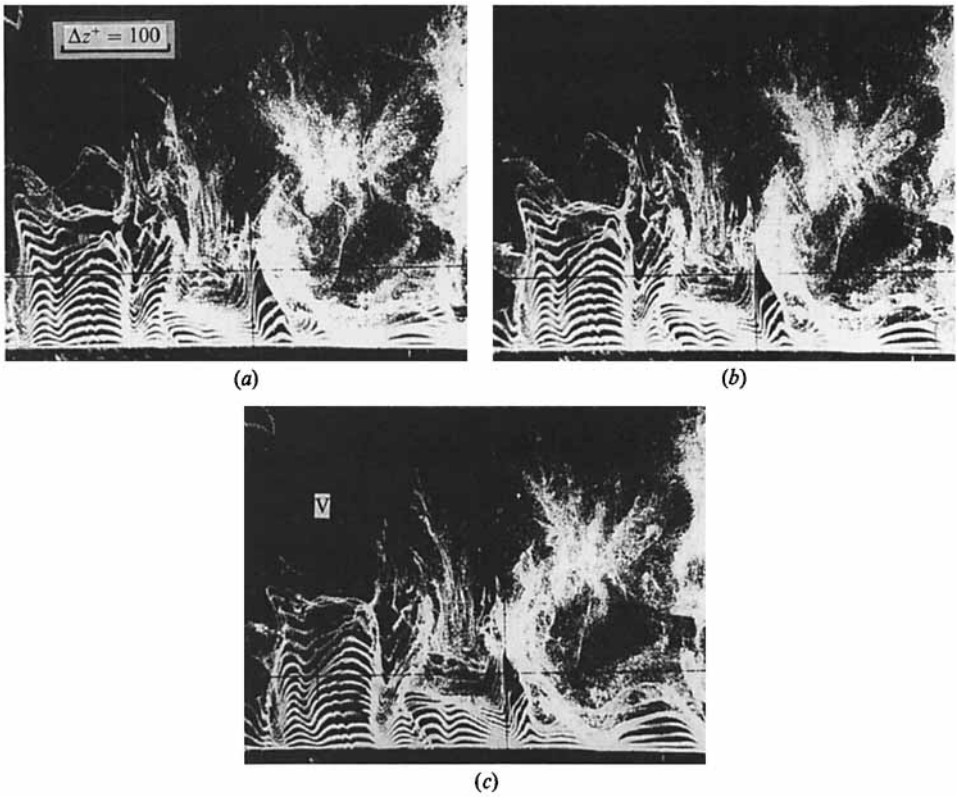

FIGURE 18. A z-vortex (transverse) at the front of a high-speed region, marked V, with both its ends linked to the lateral interfaces of its following high-speed streak, and the bubble lines in these interfaces are folding. $x = 300$ mm, $y^+ = 11$: (*a*) $t = 0.9375$ s, (*b*) 1.3125 s, (*c*) 1.4375 s.

in figures 17(*a*) to 17(*d*). The winding of these hydrogen bubble lines forms a transverse-vortex shape, and this formation of a transverse vortex shape at the front of a high-speed region can be observed frequently in the plan views.

3.6. *The hairpin vortex*

The importance of the hairpin vortex had been suggested by many authors (Theodorsen 1952; Head & Bandyopadhyay 1981; Perry, Henbest & Chong 1986; Kim & Moin 1986), yet its measurement by the usual fixed probes has not been possible since the vortex is moving. The visualization of Head & Bandyopadhyay (1981) using a smoke–laser light sheet might have been convincing evidence of the existence of hairpin vortex. However, the near-wall region was blurred by the smoke, and a complete view of the vortex was therefore lacking. Visualization of a complete hairpin vortex in a fully developed turbulent boundary layer is difficult. An incomplete view of such a vortex might perhaps be seen in a plan view using hydrogen bubble markers. Figure 18 shows the transverse vortex(z-vortex), marked V at the front of a high-speed region. This vortex is linked to the lateral interfaces of the high-speed region at both ends. The bubble lines in these lateral interfaces are folding. The folding of bubble lines along the interface region might imply an (x, y)-vortex as discussed later in §3.7, or this figure might be an incomplete view of a hairpin vortex (a z-vortex with its two ends linked to two (x, y)-vortices thus forms

a hairpin shape). It should be repeated that such complete hairpin-like shapes are rare; what appear to be tilted streamwise vortices along one leg are much more commonly seen in the pictures.

3.7. *Further discussion of long streaks and streamwise vortices*

Each hydrogen bubble gradually dissolves into the water after it has been released from the platinum wire. Therefore, the lifetime of bubble markers is limited, and should be approximately proportional to the diameter of the bubble. However, the lifetime of the hydrogen bubbles in a long streak, or in a streamwise vortex, is much longer than those in the high-speed streaks, and even longer than the lifetime of bubbles in some low-speed streaks. This can be seen from the plan views using method B of §3.3, as shown in figures 7 and 8. Since all hydrogen bubbles were released with the same time intervals, we need to ask, why do the hydrogen bubbles in the long streaks, apparently caught in streamwise vortices, exist along after all bubbles in the high-speed streaks have vanished ? If dissolving rates were augmented by high speed, then the bubbles in the region with highest speed would dissolve fastest, but they do not. The velocity of the long-streak, or the streamwise vortex, is even higher than the high-speed streak, as shown in §3.3, and in these regions the bubbles last longer. The action of a vortex is like a centrifuge; the lighter material should be drawn to the vortex centre by the radial pressure gradient. Thus the core of a vortex has concentrated hydrogen bubbles. Therefore the water in the core region should have a higher concentration of hydrogen. This slows down the solution of the bubbles into the water. Hence, the lifetime of the hydrogen bubbles becomes longer. But the reason for the concentration of hydrogen bubbles in the long streaks is not clear yet. Perhaps some of the long streaks might be an incompletely visualized streamwise vortex.

Generally, in the plan views only a small number of streamwise vortices can be observed. The hydrogen bubble time-lines can show the shape of a streamwise vortex only when they are close enough to the vortex core and also the circulation of the vortex is strong enough, so that the hydrogen bubbles can revolve through a very large angle before they vanish in the downstream direction. As shown schematically in figure 19(*b*), the platinum wire and the vortex axis are located almost in the same plane parallel to the wall, the bubble lines revolve through a large angle, and a vortex shape is seen in the plan view. When the rotation speed is low, the bubble lines rotate through a small angle as shown in figure 19(*a*), folding of bubble lines may appear in plan view, but cannot appear as a vortex shape. In the observations, about one half of the interfaces between high-speed and low-speed streaks have folding hydrogen bubble time-lines, and the long streaks generally extend from these folding interfaces, as shown in figures 13, 17 and 18. This does not mean that all these folding interfaces are incompletely visualized (x, y)-vortices; but perhaps some of them are.

The folding motion entrains the fluid from both low- and high-speed streaks to the interface region. Thus the fluid in a long streak, or in an (x, y)-vortex, should be composed of the fluid from the neighbouring streaks. Thus in the plan views visualized by method B, the velocity of its leading downstream end should approximately equal the velocity in the neighbouring high-speed streak, and the velocity of its following upstream end should approximately equal the velocity in the neighbouring low-speed streak. In the plan views, visualized by the methods described in §3.3, as shown in figures 6 to 8, the latter is approximately true, but the downstream end of the long streaks, or of the streamwise vortices, typically has a velocity greater than the velocity of neighbouring high-speed streaks. The most

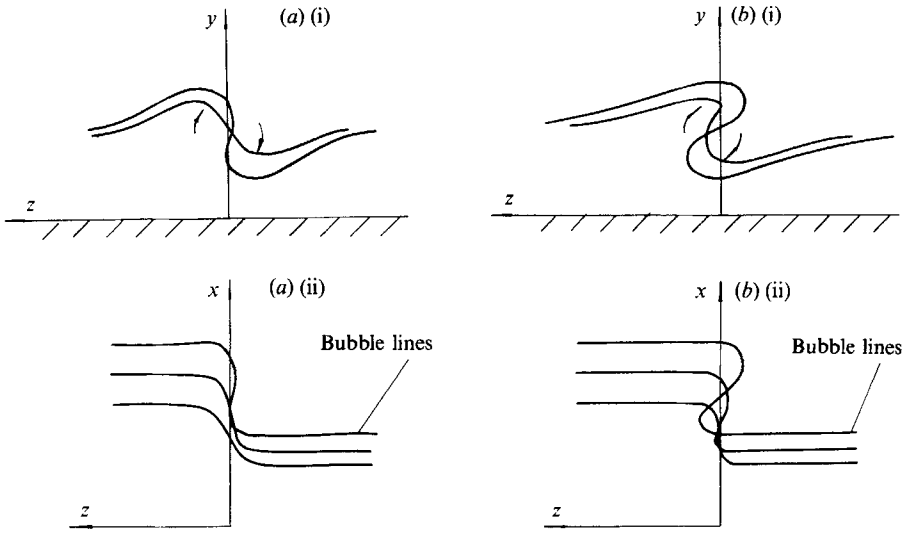

FIGURE 19. A sketch of the projection of the transverse hydrogen bubble time-lines on the plan view in the vicinity of a vortex. (*a*) The rotated angle is small, (*b*) the rotated angle is large; (i) is the end view, (ii) is the plan view.

plausible reason for the unexpectedly high speed of these downstream ends seems to be that the long streaks and the streamwise vortices are inclined to the wall, their downstream ends are farther from the wall, and thus have greater velocities.

In order to observe whether the long streaks and the streamwise vortices are actually farther from the wall at their downstream end, and also to observe the cross-section of the (x, y)-vortex and the long streaks, a method was developed, which can show the plan view, and the cross-section of the (x, y)-vortices and long streaks simultaneously on a photograph. These views were visualized by a laser light sheet inclined at 45° to the wall, normal to the (x, y)-plane, and inclined to the upstream as sketched in figure 20. Some of the motion pictures taken by this method are shown in figure 21. In these photos the straight white lines at the downstream end of the plan view and parallel to the z-axis are the intersection lines of the laser light sheet with the surfaces of the test plate, it corresponds to the line LL sketched in figure 20. The dense white marks are the hydrogen bubbles illuminated directly by the laser light sheet; they are the intersection of the hydrogen bubbles in the usual plan view with the laser light sheet. They are much brighter than the other parts of the plan view. By this technique both the usual plan view and the cross-section (cut by the laser light sheet) of the plan view can be observed in one photo as shown in figure 21. As sketched in figure 20, the distance of the mark illuminated by the laser light to the straight line LL equals the height of the hydrogen marks. By this method it is possible to obtain the cross-sections of the structures in the plan view, to locate their positions relative to the structures appeared in the plan view, and measure the heights of the structures (the long streaks, low-speed streaks, high-speed streaks, and vortices). But generally the laser light reflected and dispersed from the directly illuminated hydrogen bubbles and reflected from the plate brightened the plan view too much. Thus the contrast between the directly illuminated marks and the usual plan view was poor in the photographs. There are certain difficulties in recognizing a directly illuminated mark and locating its position in the plan view simultaneously.

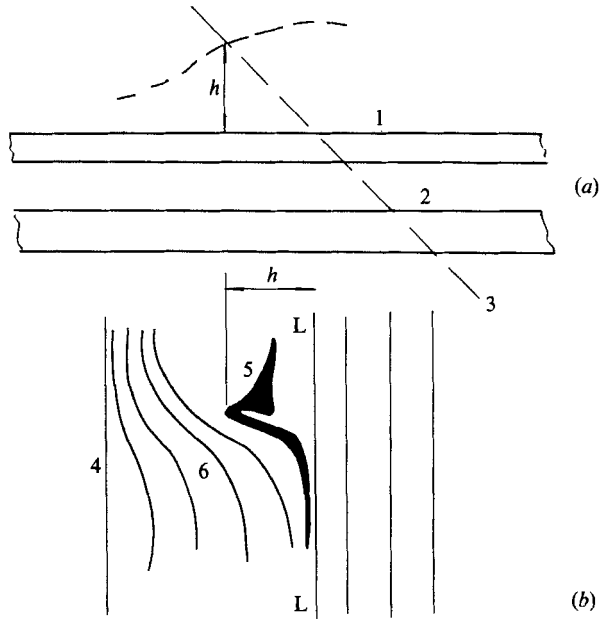

FIGURE 20. Sketch of the arrangement of the oblique laser light sheet, and the projection of the hydrogen bubble marks illuminated by the light. (*a*) The side view, (*b*) the plan view: (1) the flat plate, (2) the sidewall of the water channel, (3) the laser light sheet, (4) the platinum wire for generating hydrogen bubble time-lines, (5) the intersection of the hydrogen bubble lines with the laser light sheet (projection on the plan view), (6) the hydrogen bubble time-lines.

This difficulty was overcome by printing two photos from one film; one with the usual exposure and the other with much longer exposure. Thus the former shows the usual plan view and the laser light intersected marks; although the marks are not very clear, their position can be located in the plan view. The latter photo can show clearly the cross-section of the structures (vortices and streaks) cut by the laser light sheet, and their height can be observed. In figure 21, there are photos printed by this method. In each pair, the upper one is printed by usual exposure and the lower one is printed with long exposure. From these photos one can see most of the long streaks and the (x, y)-vortices are much higher than the high-speed streaks. The low-speed streaks are generally lifted from the wall, yet the markers lifted to the greatest heights are generally in the long streaks or the (x, y)-vortices in the interface regions. Figure 21 shows a typical observation: a wide low-speed streak is much lower than a vortex or long streak in the interface region. From the photos visualized by this method, the heights (in wall units) of the long streaks or (x, y)-vortices at station cut by the laser light sheet are of the order of around 50 to 90. The heights of the high-speed streaks are only about the order of 8, meaning that the fluid in the high-speed streaks moves parallel to the wall, as the platinum wire is also at $y^+ = 8$. In figure 21 (*b*), there is a spiral shaped vortex; it is the cross-section of an (x, y)-vortex along an interface between a low-speed and high-speed streak. This provides evidence that an (x, y)-vortex may exist in the interface region. The spiral shaped vortex sheet generally appears while the markers are rolling up. This might be evidence that some (x, y)-vortices may be growing along the interface regions. The concentration of hydrogen bubbles in the core of this spiral vortex could also be observed. In the motion picture films obvious vortex shapes do not appear as frequently as the long

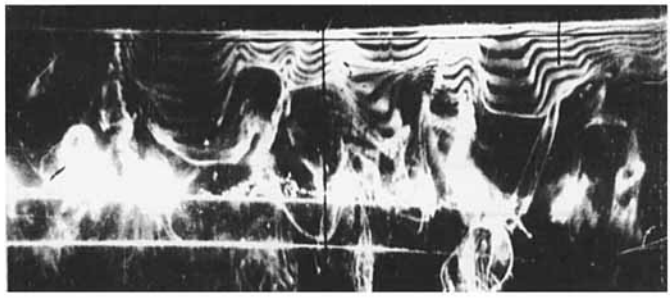

(*a*) (i)

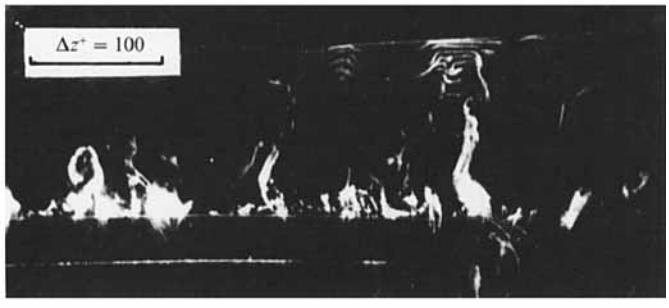

(*a*) (ii)

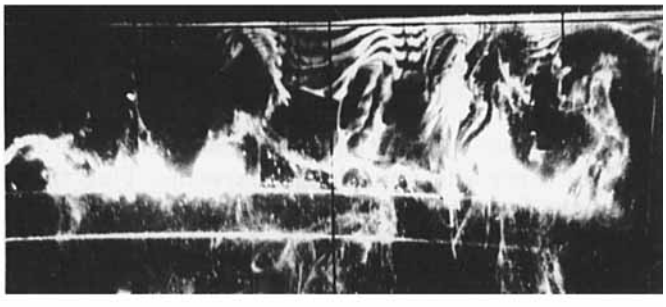

(*b*) (i)

(*b*) (ii)

FIGURE 21. Photographs show simultaneously structures illuminated by the oblique laser light sheet and the plan views at $x = 300$ mm and $y^+ = 8$. (*a*) An example of the lift-up of the interfaces with long streaks at the downstream end of the plan view. (*b*) An example of the rolled-up spiral shape vortex along an interface between a high-speed and low-speed streak: (i) denotes a photo developed with shorter exposure, (ii) denotes a photo developed with long exposure.

streaks in the interface regions. Also what appears to be growing vortices can be observed from the films; the growth is generally rather fast, and occurs only for a short time.

4. Conclusion

The lateral interface regions between high- and low-speed streaks seem to play an important role in forming streamwise vortices and in producing long streaks of marker bubbles. The reason why the long streaks have a speed even greater than the high-speed streaks seems to be that the bubbles concentrated in it continue to higher y-values, and thus are moving faster. Since bubbles concentrate in this region, the solution into water is slowed, thus explaining the persistence of the bubbles. The simple methods described in §3.3 are effective for visualizing the stretching and forming process of the long streaks and the stretching of the streamwise vortices.

The inclined laser sheet method may be useful in observing the cross-section of the plan-view structures (streaks and vortices) and finding the locations and heights of the structures simultaneously in one photograph. This method provides some evidence that the long streaks and the (x, y)-vortices are generally farther from the wall in the downstream direction. The visualized spiral shaped vortex shape may be evidence that there existed growing (x, y)-vortices along the interface regions.

In the divergent passage the boundary-layer thickness is about 50 mm to 100 mm in the region from $x = 100$ mm to 500 mm. The long streaks are very abundant in the plan views close to the wall ($y^+ \leqslant 10$). The long streaks are generally extended in the downstream direction from the folding bubble lines along the interface regions. In the plan views at $y^+ \sim 10$–20, streamwise vortices (x, y-vortices) along interface regions and transverse vortices (z-vortices) at the front of high-speed regions are frequently observed. A transverse vortex seen at the front of a high-speed region generally has one end linked to the folding bubble lines at the lateral interface of the following high-speed streak. Rarely, both ends of the z-(transverse) vortex are linked to the folding bubble lines, thus forming a hairpin-like shape as shown in figure 18(*c*). This hairpin-like shape appears very similar to the structure obtained in numerical calculations by Moin & Kim (1985, figure 13). The appearance of such a figure is rather rare in plan view. This may be due to the limitation of the hydrogen bubble method, or it may be that the regular shape of a hairpin vortex with two symmetric legs is rare in fully developed turbulent boundary layers. Nevertheless, these results may be helpful for understanding where and how these vortices exist.

The author wishes to thank Y. M. Yuan and Z. Huang, and also Miss Y. Fu for their helpful works, and also to thank the Chinese National Natural Science Foundation for the support of this research.

REFERENCES

BLACKWELDER, R. F. & CHANG, S. I. 1986 *AIAA Paper* 86-0287.

BUSHNELL, D. M. 1983 *AIAA Paper* 83-0227.

CANTWELL, C. T. 1981 *Ann. Rev. Fluid Mech.* **13**, 457.

FALCO, R. E. 1977 *Phys. Fluids* **20**, 124.

GUEZENNEC, Y. G. & NAGIB, H. M. 1985 *AIAA Paper* 85-0519.

HEAD, M. R. & BANDYOPADHAYAY, P. 1981 *J. Fluid Mech.* **107**, 197.

HUSSAIN, A. K. M. F. 1983 *Phys. Fluids* **26**, 2816.

JOHANSON, J. B. & SMITH, C. R. 1986 *AIAA J.* **24**, 1081.

KIM, J. 1983 *Phys. Fluids* **26**, 2088.

KIM, J. & MOIN, P. 1986 *J. Fluid Mech.* **162**, 339.

KLINE S. J. & FALCO, R. E. 1980 *AFOSR TR*-80-0290, ADA 083717.

KLINE, S. J., REYNOLDS, W. C., SCHRAUB, F. A. & RUNDSTADLER, P. W. 1967 *J. Fluid Mech.* **30**, 741.

LIAN, Q. X. 1983 *Acta Mechanica Sinica* **4**, 414 (in Chinese).

LIAN, Q. X. 1985 *Acta Mechanica Sinica* **1**, 71 (English edition).

MOIN, P. & KIM, J. 1985 *J. Fluid Mech.* **155**, 441.

NAKAGAWA, H. & NEZU, I. 1981 *J. Fluid Mech.* **104**, 1.

PERRY, A. E., HENBEST, S. & CHONG, M. S. 1986 *J. Fluid Mech.* **165**, 163.

SANDBORN, V. A. & KLINE, S. J. 1961 *Trans. ASME* D: *J. Basic Engng* **83**, 317.

SIMPSON, R. L., CHEW, Y. T. & SHIVAPRASAD, B. G. 1981 *J. Fluid Mech.* **113**, 23.

SIMPSON, R. L., STRIKLAND, J. H. & BARR, P. W. 1977 *J. Fluid Mech.* **79**, 553.

SMITH, C. R. & METZLER, S. P. 1983 *J. Fluid Mech.* **129**, 27.

STRATFORD, B. S. 1959 *J. Fluid Mech.* **5**, 17.

THEODORSON, T. 1952 *Proc. 2nd Midwestern Conf. on Fluid Mechanics, Ohio State University, Columbus, Ohio.*